Talanta 114 (2013) 17–24

Contents lists available at ScienceDirect

Talanta

journal homepage: www.elsevier.com/locate/talanta

Simultaneous and automated monitoring of the multimetal biosorption processes by potentiometric sensor array and artificial neural network

D. Wilson [a], M. del Valle [a], S. Alegret [a], C. Valderrama [b], A. Florido [b,*]

[a] Sensors and Biosensors Group, Chemistry Dept., Universitat Autònoma de Barcelona, 08193 Bellaterra, Barcelona, Spain
[b] Departament d'Enginyeria Química, Universitat Politècnica de Catalunya, 08028 Barcelona, Spain

ARTICLE INFO

Article history:
Received 22 October 2012
Received in revised form
16 March 2013
Accepted 25 March 2013
Available online 30 March 2013

Keywords:
Grape stalk wastes
Heavy metals sorption
Ion-selective electrodes
Electronic tongue
On-line monitoring
Fourier transform

ABSTRACT

In this communication, a new methodology for the simultaneous and automated monitoring of biosorption processes of multimetal mixtures of polluting heavy metals on vegetable wastes based on flow-injection potentiometry (FIP) and electronic tongue detection (ET) is presented. A fixed-bed column filled with grape stalks from wine industry wastes is used as the biosorption setup to remove the metal mixtures from the influent solution. The monitoring system consists in a computer controlled-FIP prototype with the ET based on an array of 9 flow-through ion-selective electrodes and electrodes with generic response to divalent ions placed in series, plus an artificial neural network response model. The cross-response to Cu^{2+}, Cd^{2+}, Zn^{2+}, Pb^{2+} and Ca^{2+} (as target ions) is used, and only when dynamic treatment of the kinetic components of the transient signal is incorporated, a correct operation of the system is achieved. For this purpose, the FIA peaks are transformed via use of Fourier treatment, and selected coefficients are used to feed an artificial neural network response model. Real-time monitoring of different binary (Cu^{2+}/ Pb^{2+}), (Cu^{2+}/ Zn^{2+}) and ternary mixtures (Cu^{2+}/ Pb^{2+}/ Zn^{2+}), (Cu^{2+}/ Zn^{2+}/ Cd^{2+}), simultaneous to the release of Ca^{2+} in the effluent solution, are achieved satisfactorily using the reported system, obtaining the corresponding breakthrough curves, and showing the ion-exchange mechanism among the different metals. Analytical performance is verified against conventional spectroscopic techniques, with good concordance of the obtained breakthrough curves and modeled adsorption parameters.

1. Introduction

Heavy metals are one of the most harmful pollutants to different ecosystems and human health. Therefore they require special attention, both control and treatment of heavy metals in different waste leads to use of expensive and complex methodologies [1,2].

Our group has studied the biological materials as bioaccumulators of heavy metals. The grape stalks generated from wine industrial wastes have taken a key role in this sense. In recent years, several works have demonstrated the ability of grape stalk wastes as good sorption material for the removal and recovery of metal ions, such as: Cu^{2+}, Cd^{2+}, Pb^{2+}, Ni^{2+}, Cr(VI) and Cr^{3+} [3–5]. Previous experiments in fixed-bed column configuration indicated that the sorption of heavy metals on grape stalks released alkaline and alkaline earth metals (K^{+}, Mg^{2+}, Ca^{2+}), as well as protons [6], suggesting that ionic exchange is predominantly responsible for metal ion uptake.

In the monitoring of metal biosorption processes, conventional analytical methods have been traditionally used, as flame atomic absorption spectroscopy (FAAS), inductively coupled plasma optical emission spectrometry (ICP-OES) and flow injection analysis with potentiometric detection (FIP) [7]. However, the limitations of these methods, the need to seek new alternatives adaptable to the study of more complex processes, specifically in multimetal mixtures and in unconventional circumstances, have led us to consider other viable alternatives such as detection with the use of sensor arrays, or electronic tongues (ET) [6].

Considering an ET as a multisensor system combined with advanced mathematical procedures for signal processing [8], the purpose of the latter differs depending on the application. If the goal is qualitative, Principal Component Analysis (PCA) is the most commonly used method, to visualize if the samples can be separated in classes (classified), or to identify a specific variety [9–11]. When the purpose is a quantitative analysis, different tools may be used; these include: principal component regression (PCR), partial least squares (PLS) or Artificial Neural Networks (ANNs) [11–14].

* Correspondence to: Departament d'Enginyeria Química, Universitat Politècnica de Catalunya, Av. Diagonal 647, 08028 Barcelona, Spain. Tel.: +34 93 4010981; fax: +34 93 401 58 14.
E-mail address: antonio.florido@upc.edu (A. Florido).

0039-9140/$ - see front matter © 2013 Elsevier B.V. All rights reserved.
http://dx.doi.org/10.1016/j.talanta.2013.03.066

The greatest advantage of using a sensor array is its ability to generate multivariate analytical data in real time and simultaneously to permit tackling the identification of interferents and the compensation of matrix effects [15]. These advantages have provided ETs with encouraging results in the monitoring of numerous processes, viz. in the industrial, clinical and environmental fields, especially in the resolution of multicomponent mixtures [15,16]. Several works of these applications stand out in the literature; Gutiérrez et al. used a sensor array formed by potentiometric sensors for the monitoring of NH_4^+, K^+, NO_3^- nutrients and Na^+, Cl^- contaminants in a fertigation solution for greenhouse cultivation [17]. Other applications associated to farming activities can be found in the work by Chang et al., related to the monitoring of water quality in fish farms which employed a screen-printed electronic tongue formed by 8 potentiometric sensors [18]. Multisensor arrays have been used as electronic tongues in the classification of mineral waters [19]. However, there are few references where an electronic tongue has been employed for simultaneous quantification of different metal ions in liquid samples [20]. Even though several authors in different types of samples have demonstrated the determination of trace heavy metals using ETs, [21,22] their use in the simultaneous monitoring and discrimination of heavy metal mixtures in industrial processes is scarce.

By integrating a flow analysis system with an electronic tongue, obvious advantages can be seen: as among others, automation, simultaneous determination and analysis in series. Several researchers have reported work leveraging this valuable tool [6,22–24]. Especially, dynamic components of the sensors' signal can be exploited and incorporated in the data treatment to help achieving a better performance from the ET system [13].

The final goal of this work is to develop a fully-automated system and analytical methodology for the simultaneous and real-time determination of heavy metals considered to be pollutants in environmental samples, employed during their removal and recovery via biosorption processes. Considering the complexity of the multimetal samples, as well as the effluent media, the combination of flow-injection techniques and electronic tongue detection (ET–FIP) is considered to be a satisfactory approach for the final objective of the monitoring of a biosorption process. Thus, biosorption of binary and ternary mixtures of divalent heavy metals using grape stalk wastes as the sorbent material implemented in a laboratory-scale fixed bed column is evaluated.

The real-time monitoring of the trace metals exchanged and the released ion (Ca^{2+}) in the effluent solution was therefore achieved by a potentiometric sensor array in conjunction with the ET–FIP system. Multidimensional transient information obtained from the flow-injection potentiometric electronic tongue system was treated with advanced chemometric tools such as an ANN, and methods of signal pre-processing such as the Fourier transform, with the ultimate goal of characterizing sorption properties against mixtures of heavy metals.

2. Experimental

2.1. Reagents and materials

The ionophores, calcium bis[4-(1,1,3,3-tetramethyl-butyl)-phenyl]-phosphate (CaBTMBPP), calcium-ionophore I (ETH 1001), tetrabenzyl pyrophosphate (TBPP), 1,3-bis(N-benzoylthioureido) benzene (BTB), S,S´-methylene bis(N,N-diisobutyldithiocarbamate) (MBDiBDTC), cadmium-ionophore I (N,N,N',N'-tetrabutyl-3,6-dioxaoctanedi(thioamide), TBDTA), trioctyl phosphine oxide (TOPO) and tetrabutyl thiuram disulfide (TBTDS); the plasticizers, dioctylphenylphosphonate (DOPP), 2-nitrophenyloctylether (NPOE), bis (1-butylpentyl)adipate (BBPA), (10-hydroxydecyl)butyrate (ETH 264) and dioctyl sebacate (DOS); the additive potassium tetrakis (4-chlorophenyl)borate (KTpClPB); and the polymer grade poly (vinyl chloride) (PVC) were obtained from Fluka (Buchs, Switzerland).

Stock metal solutions were prepared by dissolving appropriate amounts of their nitrate salts in deionised water (Milli-Q, Millipore; Molsheim, France). These reagents, tetrahydrofuran (THF) and metal standard solutions (1000 mg L^{-1}, used for Flame Atomic Absorption Spectroscopy, FAAS) were analytical grade and purchased from Merck (Darmstadt, Germany).

Grape stalk wastes (supplied by a wine manufacturer of Subirats, Penedès DO region, Barcelona, Spain), were rinsed and treated as in previous work [7]. A particle size of 0.8–1.0 mm was used in all experiments.

2.2. Membranes and electrodes

The tubular flow-through electrodes (ISEs) used in the ET–FIP system corresponded to all-solid-state type or non-symmetric configuration; these electrodes are based on a direct ohmic contact between the transducer and the membrane. Two types of membranes were used: heterogeneous crystalline membranes, based on a composite of Ag_2S–CuS in epoxy resin used in the preparation of the Cu^{2+}-selective sensors [7], and polymeric membrane with mobile carrier, constructed according to established procedures in our laboratories [25]. Table 1 shows the composition of the membranes used in the sensors arrays [26–33]. The ISEs were inserted in the flow system with help of a Perspex sandwich module [34]. The potentiometric measurement cell was

Table 1
Composition of the sensor membranes employed in ET–FIP.

Sensor	PVC (%)	Plasticizer (%)	Ionophore (%)	Reference
Ca^{2+} (1)	33.3	NPOE (65.2)	Calcium-ionophore I (1.0)	[23]
Ca^{2+} (2)	29.8	DOPP (63.2)	Calcium bis[4-(1,1,3,3-tetramethyl-butyl)-phenyl]-phosphate (7.0)	[24]
Pb^{2+} (1)	37.2	NPOE (49.6)	S,S´Methylenebis(N,N-diisobutyldithiocarbamate) (11.2)	[25]
Pb^{2+} (2)[a]	33.0	DOS (61.5)	1,3-bis(N-benzoylthioureido)benzene (5.0)[b]	[26]
Zn^{2+}	40.2	NPOE (53.6)	Tetrabutyl thiuram disulfide (5.3)[b]	[27]
Cd^{2+}	34.0	ETH 264 (65.0)	Cadmium-ionophore I (1.0)[b]	[28]
Generic (1)	34.5	BBPA (63.2)	Tetrabenzyl pyrophosphate (2.3)[b]	[29]
Generic (2)	37.7	NPOE (54.9)	Trioctyl phosphine oxide (5.2)[b]	–
Cu^{2+}	CuS (30.9%), Ag_2S (30.9%), Araldite M (27.2%) and HR hardener (10.9%)			[30]

[a] Ionophore not commercially available.
[b] The formulation included potassium tetrakis(4-clorophenyl)borate as additive.

completed with an Orion double-junction electrode (Model 90-02-00, Thermo Fisher Scientific, Beverly, MA, USA) as reference electrode.

2.3. Sorption experiments

All sorption experiments were conducted by duplicate in glass columns of 72 mm length and 10 mm internal diameter (Omnifit), and uniformly packed with 1.3 g of grape stalk waste (particle size of 0.8–1.0 mm) previously treated. During the column sorption operation, different binary and ternary mixtures composed by Cu^{2+}, Pb^{2+}, Zn^{2+} and Cd^{2+} ions in deionised water were prepared. The following metal combinations (Cu^{2+} and Pb^{2+}), (Cu^{2+} and Zn^{2+}), (Cu^{2+}, Cd^{2+} and Zn^{2+}) and (Cu^{2+}, Pb^{2+} and Zn^{2+}) were studied, employing 5.5×10^{-4} mol L^{-1} approximate concentration of each metal. In the sorption experiment, each metal mixture was pumped upwards through the column at a constant flow rate (30 mL h^{-1}). The sorption of metals from these mixtures involved ion-exchange processes where Ca^{2+}, H^+ and other ions, present in the grape stalks, were released [3,5,6]. The input solution in the column sorption consisted in the binary and ternary combinations mentioned above, and the effluent outlet of the column was composed by a solution with variable content of Ca^{2+}, as well as other ions (H^+, K^+, etc.) released in lower amounts. When the outlet concentration achieved the input concentration, the column was considered as saturated.

For the sorption monitoring experiment, the column effluent was sampled at fixed time intervals, and brought to the sensor array, in order to determine the concentration of the analytes vs. process time. Additionally, in order to compare obtained results with conventional analytical techniques, samples were collected from the outlet of the column employing a fraction collector (Gilson FC204) at pre-set time intervals. Each effluent metal concentration was determined by FAAS, at its corresponding wavelength, by using a Varian Absorption Spectrometer (Model 1275) and, in the case of Ca^{2+}, by ICP-OES (Perkin-Elmer model Optima 4300DV). All experiments were performed at room temperature.

2.4. Breakthrough sorption capacity

The capacity at exhaustion q_0 (mmol g^{-1}) is determined by using the graphical integration of the area above the breakthrough curve. This area represents the amount of solute sorbed by mass of solid in the sorption zone that goes from the breakpoint to exhaustion [3,4].

The breakthrough point is chosen arbitrarily at some low value, C_b (mmol L^{-1}); and the sorbent is considered to be essentially exhausted when the effluent concentration, C_x (mmol L^{-1}), reaches the 95% of C_0 (initial concentration of sorbate, mmol L^{-1}) [35,36].

$$q_0 = \frac{\int_{V_b}^{V_x}(C_0 - C)dV}{m} \quad (1)$$

where V_b and V_x (L) are the volumes of liquid passed through column at breakthrough and exhaustion respectively, C is the outlet metal concentration (mmol L^{-1}) and m is the mass of sorbent (g).

In order to compare the values measured by ET–FIP to those determined by the FAAS and ICP-OES techniques, the relative error (RE) was used; this parameter indicates an estimation of error between the breakthrough capacity determined by both techniques and can be calculated by using the following equation [37]:

$$RE = \frac{q_{0\ \mathrm{FAAS/ICP}} - q_{0\ ET-FIP}}{q_{0\ \mathrm{FAAS/ICP}}} \quad (2)$$

2.5. Electronic tongue–flow injection experiments (ET–FIP)

A total of 9 tubular electrodes were included in the developing of the ET–FIP system (see Table 1). Two sensors with primary response to Ca^{2+} ions, two to Pb^{2+} ions, one for each of other ions (Cd^{2+}, Cu^{2+} and Zn^{2+}) and two generic sensors with general response to heavy metals (Generic (1) and Generic (2)) were employed.

In present experiments, the same hardware, software and manifold of the computer controlled-flow injection potentiometric system, as well as the monitoring procedure, flow parameters and other characteristics, developed and optimized in former works were used [6,7].

A 0.2 mol L^{-1} sodium nitrate solution was used as ionic strength adjustor. In order to improve the recovery of the baseline, a background level of the target ions was added. Thus a carrier solution with a metal total concentration of 2.0×10^{-6} mol L^{-1}, composed on equimolar nitrates salts of the ions was used in all experiments.

The nonlinear response of the sensors produced by the interference effect was modeled effectively by ANN. In the training determinations, the patterns used in the ET–FIP consisted of 27 different standard solutions mixtures of (Cu^{2+}, Pb^{2+} and Ca^{2+}), (Cu^{2+}, Zn^{2+} and Ca^{2+}), (Cu^{2+}, Pb^{2+}, Zn^{2+} and Ca^{2+}) and (Cu^{2+}, Zn^{2+}, Cd^{2+} and Ca^{2+}) prepared by dilution from a 1 mol L^{-1} stock solution of each metal. From these, an independent subset including 10 analogue solutions was employed for evaluating modeling performance of the developed methodology. The concentration levels ranged from 0 to 0.008 mol L^{-1} (0 to 320.62 mg L^{-1} for Ca^{2+}, 0 to 508.37 mg L^{-1} for Cu^{2+}, 0 to 1657.60 mg L^{-1} for Pb^{2+}, 0 to 899.28 mg L^{-1} for Cd^{2+} and 0 to 523.96 mg L^{-1} for Zn^{2+}) for all ions. ANN calculations were done in MATLAB 7.0 (MathWorks, Natick, MA) using its Neural Network Toolbox (v. 4.0).

3. Results and discussion

3.1. Sensor characterization

A complete characterization of ISEs response was performed before developing the final ET application. In this way, the main performance characteristics of prepared sensors were determined, which are summarized in Table 2.

Nernstian responses for the corresponding primary ion, with slopes around +29 mV/dec, as expected for divalent cations, were obtained for all electrodes studied. The values of the practical detection limits (PDL) were nearby to 10^{-6} mol L^{-1} for all ISEs except for Ca^{2+} (1) and Pb^{2+} (1) sensors that presented a PDL of $4.2\pm0.6\times10^{-7}$ and $1.2\pm1.1\times10^{-7}$ mol L^{-1}, respectively. The stability of the electrodes was studied during 12 weeks in practically daily different experiments; in this period the slope and PDL values for all sensors were comparable to initial values, with standard deviations (for 48 determinations) lower than ±2.1 mV/dec and $\pm1.8\times10^{-6}$ mol L^{-1} for slope and PDL, respectively.

The cross-response is an important feature of ISEs in order to develop an ET [8,38]. Thus, to estimate the cross-selectivity of the sensors used in this work, the potentiometric selectivity coefficients were determined by using the fixed interference method (FIM) [39]. By examining the values of the obtained selectivity coefficients (see Table 3), it is clear that, although using state-of-the-art membrane compositions, all sensors used showed certain cross-response to the target ions, a desirable situation to develop ET applications.

The concentration range of linear response was determined with the objective to establish the concentration limits for the calibration model and quantification of the samples. For the

Table 2
Response characteristics of the ISEs used in ET–FIP.

Principal ion	Pb^{2+}		Zn^{2+}		Ca^{2+}		Cd^{2+}		Cu^{2+}		PDL for primary ion (M)[b]
Sensor	Slope[a] (mV/dec)	Range (M)	Slope[a] (mV/dec)	Range (M)	Slope[a] (mV/dec)	Range (M)	Slope[a] (mV/dec)	Range (M)	Slope[a] (mV/dec)	Range (M)	
Ca^{2+} (1)	9.9 ± 1.9	2.1×10^{-5}; 7.0×10^{-3}	9.1 ± 2.0	3.1×10^{-5}; 8.0×10^{-3}	29.8 ± 0.9	7.5×10^{-7}; 6.5×10^{-2}	7.1 ± 2.5	4.2×10^{-5}; 9.0×10^{-3}	18.2 ± 2.1	2.2×10^{-5}; 9.0×10^{-3}	$(4.2\pm0.6)\times10^{-7}$
Ca^{2+} (2)	14.6 ± 1.8	1.4×10^{-5}; 9.2×10^{-2}	12.9 ± 2.1	2.0×10^{-5}; 5.3×10^{-3}	30.1 ± 1.1	5.7×10^{-6}; 0.5×10^{-2}	15.2 ± 2.0	5.0×10^{-5}; 9.3×10^{-3}	20.8 ± 2.1	1.7×10^{-5}; 8.1×10^{-3}	$(1.3\pm0.7)\times10^{-6}$
Pb^{2+} (1)	29.8 ± 1.9	5.0×10^{-7}; 1.0×10^{-2}	6.2 ± 2.5	7.9×10^{-6}; 5.0×10^{-3}	10.4 ± 2.2	2.3×10^{-5}; 1.0×10^{-3}	11.4 ± 1.2	5.8×10^{-6}; 8.0×10^{-3}	29.5 ± 1.4	1.0×10^{-6}; 1.0×10^{-2}	$(1.2\pm1.1)\times10^{-7}$
Pb^{2+} (2)	30.0 ± 2.1	4.2×10^{-6}; 1.0×10^{-2}	5.2 ± 2.1	5.8×10^{-5}; 5.0×10^{-3}	10.3 ± 2.4	2.7×10^{-5}; 8.7×10^{-2}	10,3 ± 2.3	8.9×10^{-5}; 8.5×10^{-3}	24. 5 ± 1.5	8.1×10^{-6}; 1.0×10^{-2}	$(9.3\pm2.3)\times10^{-7}$
Zn^{2+}	24.1 ± 2.3	7.5×10^{-5}; 5.0×10^{-3}	31.2 ± 2.4	3.2×10^{-6}; 1.0×10^{-1}	10.1 ± 1.2	8.2×10^{-5}; 2.8×10^{-3}	25.4 ± 2.2	4.2×10^{-6}; 1.0×10^{-2}	29.0 ± 2.3	4.2×10^{-5}; 1.0×10^{-2}	$(1.2\pm1.3)\times10^{-6}$
Cd^{2+}	11.2 ± 2.0	7.3×10^{-5}; 8.0×10^{-3}	5.2 ± 2.2	3.0×10^{-5}; 8.0×10^{-3}	7.8 ± 1.5	3.8×10^{-5}; 9.1×10^{-3}	29.8 ± 2.1	5.3×10^{-6}; 1.0×10^{-1}	17.7 ± 2.1	5.7×10^{-5}; 5.0×10^{-3}	$(2.1\pm1.2)\times10^{-6}$
Cu^{2+}	19.9 ± 2.3	8.9×10^{-6}; 9.0×10^{-2}	8.21 ± 1.3	3.1×10^{-5}; 8.2×10^{-3}	17.6 ± 1.2	5.1×10^{-5}; 8.9×10^{-3}	20.0 ± 1.9	1.3×10^{-5}; 5.7×10^{-3}	30.4 ± 1.3	8.6×10^{-6}; 1.2×10^{-2}	$(2.0\pm0.5)\times10^{-6}$
Generic(1)[c]	28.3 ± 1.9	1.7×10^{-5}; 1.0×10^{-2}	17.2 ± 2.5	1.5×10^{-5}; 9.7×10^{-3}	25.8 ± 1.2	2.7×10^{-5}; 8.9×10^{-3}	19.6 ± 2.5	1.5×10^{-5}; 1.0×10^{-2}	28.0 ± 1.5	6.8×10^{-6}; 1.3×10^{-2}	$(2.1\pm1.5)\times10^{-6}$
Generic (2)[d]	25.3 ± 2.5	0.5×10^{-5}; 1.0×10^{-2}	28.8 ± 2.1	8.3×10^{-6}; 9.6×10^{-3}	16.8 ± 2.1	8.8×10^{-6}; 3.5×10^{-3}	29.1 ± 1.6	1.1×10^{-5}; 1.0×10^{-2}	22.0 ± 1.5	6.8×10^{-6}; 1.3×10^{-2}	$(2.3\pm1.8)\times10^{-6}$

[a] $n=10$.
[b] $n=4$.
[c] Selected Pb^{2+} as primary ion.
[d] Selected Zn^{2+} as primary ion.

Table 3
Potentiometric selectivity coefficient values ($logK_{i,j}^{pot}$) of the ISEs used in ET–FIP.

Sensor and primary ion (i)	Interfering ion (j)				
	Ca^{2+}	Pb^{2+}	Zn^{2+}	Cd^{2+}	Cu^{2+}
Ca^{2+} (1)	–	−3.2	−2.8	−3.4	−3.2
Ca^{2+} (2)	–	−3.1	−2.5	−4.1	−2.5
Pb^{2+} (1)	−4.8	–	−3.1	−3.6	+0.7
Pb^{2+} (2)	−4.2	–	−2.4	−3.7	−1.1
Zn^{2+}	−3.8	−2.1	–	−2.6	−1.8
Cd^{2+}	−4.1	−2.8	−2.3	–	−2.5
Cu^{2+}	−3.5	−1.8	−2.3	−4.1	–

studied electrodes, the values ranged between 5.0×10^{-7} and 1.0×10^{-1} mol L^{-1} (see Table 2).

In previous studies, a complete optimization of the system was performed [7] and the influence of flow rate and injection time in the response of a 5 sensor array was verified [6]. This work was developed under the same conditions, with exception, besides the number of the array sensors, in the composition of the carrier solution. As it was mentioned above, a carrier solution containing equimolar amount of each target ions with total concentration of 2.0×10^{-6} mol L^{-1} was employed; the goal of this is to accelerate FIA recovery times after injection.

3.2. Building of the ANN response model

Artificial Neural Networks (ANNs) were used as the mathematical method of data processing, in order to build the response model for every case considered in this work. A total of 27 solutions for inlet binary mixtures of Cu^{2+} and Pb^{2+} (plus Ca^{2+}), and Cu^{2+} and Zn^{2+} (plus Ca^{2+}) and inlet ternary mixtures of Cu^{2+}, Pb^{2+} and Zn^{2+} (plus Ca^{2+}) and Cu^{2+}, Zn^{2+} and Cd^{2+} (plus Ca^{2+}) were prepared in order to achieve the model response. The selection of the concentration of the ions employed in the training subset was prepared by a complete factorial design with 3 levels of concentration and 3 ions (factors) for the inlet binary mixtures (plus Ca^{2+}). However, a fractional factorial design, with 3 levels of concentration and 4 ions (factors) was used for inlet ternary mixtures (plus Ca^{2+}).

Also, 10 additional synthetic samples, defined randomly but within the expected concentration range, were included in a test subset for evaluating the model's predictive ability. The choice is done avoiding having samples with maxima or minima in the testing subset, in order to eliminate any extrapolation [40].

From the experience obtained in previous work [41], the following characteristics of the ANN were initially fixed, done before starting the optimization process: the type of network (feedforward, backpropagation with multiple output), the training algorithm (Bayesian regularization), the training parameters (learning rate, $\alpha=0.1$, and momentum, $\beta=0.4$), and the use of a single hidden layer. In order to obtain a certain level of confidence in the final results, other configuration parameters were optimized such as the number of neurons in the hidden layer, and the transfer functions in the hidden and output layers (tested *logsig*: log-sigmoidal, *tansig*: hyperbolic tangent sigmoid, *purelin*: linear *and satlins*: saturated-linear). The best combination of the ANN configuration was selected from the root mean square error (RMSE) and prediction abilities obtained by the predicted vs. expected comparison graphs for all target metals.

3.3. Optimization of ANN model

The selection of the appropriate parameters for the data processing was one of the difficulties due to the complexity of

the multidimensional signal obtained. The optimization process was performed initially considering the peak height as input signal to the ANN, as done in previous experiments [6]. Unfortunately, in this first approach, a large dispersion for all optimization parameters (RMSE, slope, regression coefficient and intercept) was observed, that prevented to develop a proper response model. To improve the performance of the approach, the dynamic components of the sensors' signals were incorporated in the response model [13,40]. For this purpose, a pre-treatment of the recorded transient signal was then employed, in which the Fourier transform was applied and a compression approach attempted. Therefore, in order to get the best final performance, the number of lower frequency Fourier coefficients used to represent each sensor signal was included as another optimized variable. In all cases, a total number of 384 arrangements were tested, and run in fivefold, in order to optimize the ANN configuration (12 neuron numbers $\times$ 4 transfer function combinations $\times$ 8 Fourier coefficient ranges).

3.4. ANN optimization for the monitoring of binary mixtures

Two binary mixtures were evaluated, the first contained (Cu^{2+} and Pb^{2+}) and the other (Cu^{2+} and Zn^{2+}), including in both cases the measurement of the Ca^{2+} release from the biosorbent. In the first experiment, the monitoring of Cu/Pb/Ca mixture, 7 ISEs were included in the ET (see Table 1): five with primary response to the target ions and two with generic response. The best model was obtained for one Fourier coefficient, 7 neurons in the input layer (7 ISEs $\times$ 1 coefficient), 4 in the hidden layer and 3 in the output layer (one per analyte), and the *tansig* (hyperbolic tangent sigmoid) transfer function was used both in the hidden and output layer. In the monitoring of Cu/Zn/Ca system, 7 ISEs were also included in the ET, four with primary response to the target ions, two generic ISEs and one replica of the Zn^{2+} electrode. Also in this case, the best model was obtained for the same ANN topology. In the case of binary mixtures, as the use of one single Fourier coefficient is sufficient, it can be deduced that the dynamic components of the signal are not necessary, and the response model is just developed from the mean of the sensor response (peak height).

3.5. ANN optimization for the monitoring of ternary mixtures

Two ternary mixtures, (Cu^{2+}/Pb^{2+}/Zn^{2+}) and (Cu^{2+}/Zn^{2+}/Cd^{2+}), as well as the release of Ca^{2+} from the grape stalk wastes were also studied. The monitoring of Cu/Pb/Zn/Ca system needed a 9 ISEs sensor array (see Table 1). The conditions selected for the best model were: 4 Fourier coefficients, 36 neurons in the input layer (9 ISEs $\times$ 4 coefficients), 10 neurons in the hidden layer and 4 in the output layer (one per analyte), the *tansig* transfer function was used in both, the hidden and output layer. The Cu/Cd/Zn/Ca mixture was performed by using an ET based on 9 ISEs, the 7 previously employed for Cu/Zn/Ca plus a Cd^{2+} sensor with a replica. The best conditions found were: 3 Fourier coefficients, 27 neurons in the input layer (9 ISEs $\times$ 3 coefficients), 8 neurons in the hidden layer and 4 at the output layer (one per analyte), and the transfer functions, *tansig* and *purelin* for the hidden and output layers, respectively.

In Table 4, the obtained performances for the four mixtures studied are summarized. Comparison graphs of predicted vs. expected concentrations were constructed for the different metals considered. The linear regression results between the obtained (y) and expected (x) concentrations, as well as the RMSEs values for the training and external test subsets are presented. In the correlation analysis, all confidence intervals were calculated at the 95% confidence level. One can observe that the model prediction is satisfactory for all mixtures, with slope values, intercepts and correlation coefficients close to the theoretical diagonal line: 1, 0 and 1, respectively. Moreover, the prediction values, indicated by the low RMSE values, were in agreement with the above facts. It is important to point out that in most cases the results for the monitoring of inlet binary (plus Ca^{2+}) mixtures presented lower errors than inlet ternary (plus Ca^{2+}) mixtures. This circumstance is consistent with the increased complexity of monitoring experiments of 4 metals with the proposed methodology, and also with the fact that only when incorporating the dynamic component, a correct performance was attained [21].

3.6. Evaluation of the monitoring of multimetal biosorption process with ET–FIP system

In this experiment, a laboratory-scale fixed-bed column filled with grape stalk wastes was connected to the ET–FIP system in order to study the biosorption process of the four heavy metal combination mixtures, as well as the subsequent release of Ca^{2+} ions. The monitoring of the biosorption process was performed at a similar way as reported previously [7], considering that each mixture was monitored immediately after the cross calibration of the ET to avoid a possible variability on the determinations with the time. Only, in this case, the dynamic components of the sensor signal were incorporated in the response model, as extracted by the Fourier transform, as the way to resolve the most intricate mixtures.

Table 4
Obtained performances for the four optimized study cases: the binary inputs (Cu^{2+}/Pb^{2+}) and (Cu^{2+}/Zn^{2+}), and the ternary mixtures (Cu^{2+}/Pb^{2+}/Zn^{2+}) and (Cu^{2+}/Zn^{2+}/Cd^{2+}).

Training subset					External test subset			
Ion	Slope	Intercept (mM)	R^2	RMSE (mM)	Slope	Intercept (mM)	R^2	RMSE (mM)
Pb^{2+}	1.015 ± 0.016	−0.003 ± 0.054	0.999	0.018	1.050 ± 0.055	−0.023 ± 0.235	0.978	0.051
Cu^{2+}	1.014 ± 0.019	−0.003 ± 0.049	0.998	0.003	1.048 ± 0.084	−0.021 ± 0.328	0.957	0.069
Ca^{2+}	1.020 ± 0.036	−0.002 ± 0.027	0.999	0.010	0.947 ± 0.068	0.044 ± 0.317	0.963	0.051
Zn^{2+}	1.002 ± 0.003	−0.008 ± 0.014	0.999	0.007	0.978 ± 0.254	0.042 ± 0.253	0.974	0.042
Cu^{2+}	1.001 ± 0.001	−0.002 ± 0.005	0.999	0.008	0.974 ± 0.039	−0.026 ± 0.184	0.988	0.004
Ca^{2+}	1.002 ± 0.002	−0.006 ± 0.014	0.999	0.006	1.027 ± 0.053	−0.007 ± 0.180	0.979	0.016
Pb^{2+}	1.024 ± 0.029	−0.010 ± 0.040	0.998	0.031	0.955 ± 0.110	0.060 ± 0.311	0.958	0.070
Zn^{2+}	1.034 ± 0.041	−0.008 ± 0.037	0.998	0.009	0.990 ± 0.092	0.018 ± 0.209	0.971	0.072
Cu^{2+}	1.029 ± 0.038	−0.001 ± 0.034	0.999	0.022	0.991 ± 0.076	0.197 ± 0.118	0.960	0.067
Ca^{2+}	1.033 ± 0.037	−0.003 ± 0.029	0.999	0.013	0.970 ± 0.083	0.240 ± 0.023	0.975	0.065
Cd^{2+}	1.004 ± 0.008	−0.010 ± 0.039	0.999	0.013	0.945 ± 0.071	0.268 ± 0.298	0.954	0.057
Zn^{2+}	1.003 ± 0.008	−0.010 ± 0.036	0.999	0.086	0.935 ± 0.075	0.167 ± 0.394	0.959	0.099
Cu^{2+}	1.001 ± 0.001	−0.007 ± 0.004	0.999	0.012	0.968 ± 0.055	0.057 ± 0.406	0.968	0.045
Ca^{2+}	1.003 ± 0.007	−0.011 ± 0.036	0.999	0.007	1.040 ± 0.062	0.158 ± 0.252	0.968	0.032

Concentrations were therefore deduced after processing the transient FIA peak with the properly optimized Fourier-ANN coupling.

Figs. 1–4 show the breakthrough curves obtained during the monitoring of the biosorption processes with the four mixtures studied. These curves also show the comparison between the conventional methods (FAAS or ICP-OES) and the proposed method (ET–FIP) for each metal studied. Alas, we could not compare directly the concentration values obtained using the reference analytical procedures (FAAS, ICP-OES) and those with the reported ET–FIP system. This is because there are significant differences in the collection time of samples for the reference methods and the injection time corresponding to the ET–FIP system. Nevertheless, when the general profiles were examined, a good agreement was observed in all cases between the breakthrough curves obtained by the proposed method (ET–FIP) and reference methods (FAAS or ICP-OES). Also, the values of the capacity at exhaustion (q_0) for each metal and for each inlet binary or ternary mixtures for the proposed system and for the reference methods are compared in Table 5. The RE values obtained for all experiments are lower than 0.07, which evidences that there are non-significant differences between the proposed method (ET–FIP) and the reference methods (FAAS or ICP-OES). The higher RE values for Zn^{2+} in the second mixture ($RE=0.07$) can be attributed to a need of additional experimental points in the maximum biosorption zone in order to determine more precisely the q_0 values (see Fig. 1).

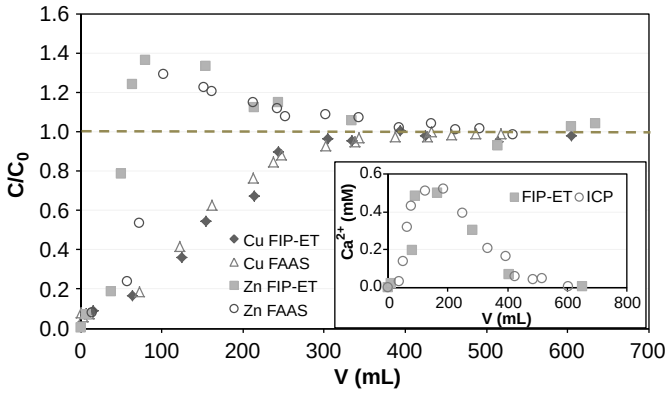

Fig. 1. The breakthrough curves for the sorption of the binary mixture Cu^{2+} and Zn^{2+} onto grape stalks obtained by the on-line ET–FIP system and by FAAS. The inserted graphic is the profile of Ca^{2+} ions obtained by the on-line ET–FIP system and by ICP-OES.

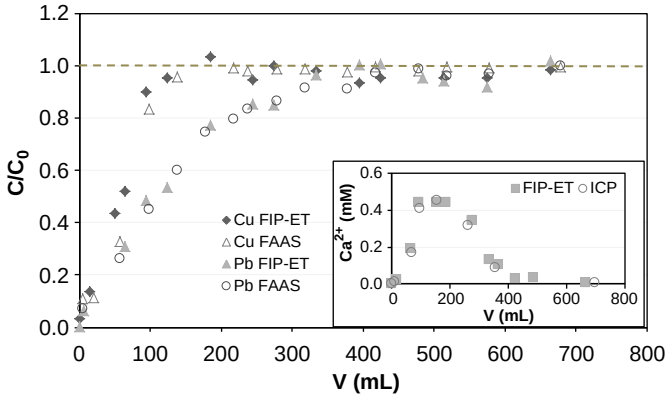

Fig. 2. The breakthrough curves for the sorption of the binary mixture Cu^{2+} and Pb^{2+} onto grape stalks obtained by the on-line ET–FIP system and by FAAS. The inserted graphic is the profile of Ca^{2+} ions obtained by the on-line ET–FIP system and by ICP-OES.

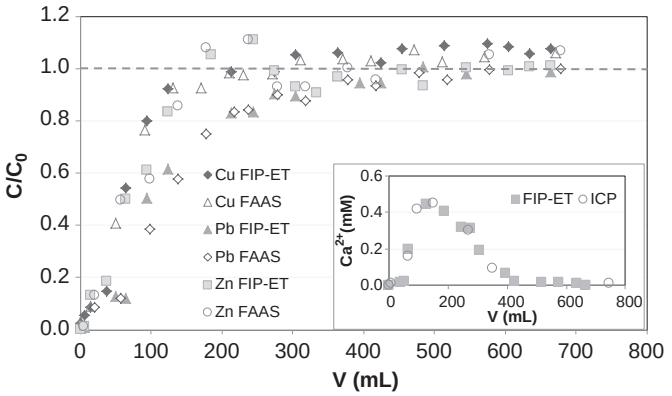

Fig. 3. The breakthrough curves for the sorption of the ternary mixture Cu^{2+}, Pb^{2+} and Zn^{2+} onto grape stalks obtained by the on-line ET–FIP system and by FAAS. The inserted graphic is the profile of Ca^{2+} ions obtained by the on-line ET–FIP system and by ICP-OES.

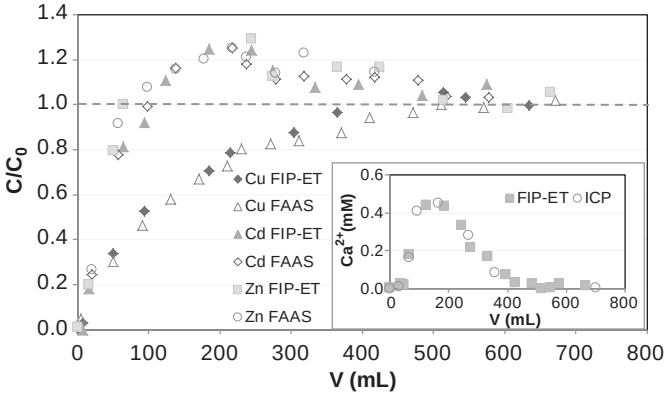

Fig. 4. The breakthrough curves for the sorption of the ternary mixture Cu^{2+}, Cd^{2+} and Zn^{2+} onto grape stalks obtained by the on-line ET–FIP system and by FAAS. The inserted graphic is the profile of Ca^{2+} ions obtained by the on-line ET–FIP system and by ICP-OES.

3.7. Sorption performance in multimetal experiments

The performance of the grape stalk wastes for binary and ternary metal sorption in fixed bed column was evaluated considering the experimental data obtained by the ET–FIP technique. The obtained breakthrough capacities of the systems are collected in Table 5.

In binary system, the concentration overshoot observed respect the expected value $C/C_0=1$ in some breakthrough curves (Fig. 1), could be caused considering the Cu^{2+} affinity for the biosorbent would be much higher than Zn^{2+} (competitive cation), causing the gradual replacement of these ions inside the column by Cu^{2+}; this phenomenon was reported in previous studies [42–47].

The selectivity of the grape stalks for Pb^{2+} over the other three metals is also demonstrated by the results obtained from the fixed bed column experiments. As can be seen in Fig. 2, Cu^{2+}, due to their low affinity compared to Pb^{2+}, broke through the column faster than Pb^{2+}. Similar behavior is observed for Cu^{2+} and Zn^{2+} in ternary system Pb/Cu/Zn (Fig. 3). Finally, Cu^{2+} showed higher affinity in front of Cd^{2+} and Zn^{2+}, as can be seen in Fig. 4 (ternary system). It is important of pointing out, that Cu^{2+} presents higher affinity in front of Zn^{2+} and Cd^{2+} (Figs. 1 and 4); however, the selectivity decreases in front of Pb^{2+} in binary system (Fig. 2) and

Table 5
Breakthrough sorption capacity.

System	Cation	FIP–ET q_0 (mmol g^{-1})	ICP/FAAS q_0 (mmol g^{-1})	*RE*
Cu/Pb/Ca	Ca^{2+}	0.067	0.064	0.03
	Cu^{2+}	0.026	0.026	0.02
	Pb^{2+}	0.070	0.067	0.05
Cu/Zn/Ca	Ca^{2+}	0.069	0.066	0.04
	Cu^{2+}	0.065	0.062	0.04
	Zn^{2+}	0.015	0.014	0.07
Cu/Pb/Zn/Ca	Ca^{2+}	0.060	0.062	0.03
	Cu^{2+}	0.033	0.033	0.02
	Pb^{2+}	0.061	0.064	0.05
	Zn^{2+}	0.029	0.031	0.05
Cu/Zn/Cd/Ca	Ca^{2+}	0.060	0.061	0.01
	Cu^{2+}	0.059	0.062	0.05
	Zn^{2+}	0.014	0.014	0.01
	Cd^{2+}	0.021	0.020	0.03

significantly in ternary system (Fig. 3), where the Cu^{2+} performance follows the Zn^{2+} pattern.

Comparing the breakthrough curves obtained in Figs. 1–4 and considering the breakthrough capacities summarized in Table 5, the affinity order of grape stalks for the four metals under study would be established as: $Pb^{2+} > Cu^{2+} > Zn^{2+} \geq Cd^{2+}$.

The release of Ca^{2+} from the grape stalk wastes was also monitored in the effluent solution in order to evaluate the sorption behavior of the exchanged cations. Results indicate the ionic exchange process as the predominant mechanism responsible for ion uptake in the biosorption process. The amounts of Ca^{2+} released expressed in mmol g^{-1} of biosorbent are collected in Table 5. It can be stated that this amount is slightly higher in binary than in ternary systems, which indicates that the exchange of Ca^{2+} ions in ternary systems can be lower due to the affinity of grape stalks for Ca^{2+} in front of overshooting metals Zn^{2+} and Cd^{2+}; this fact has already been reported for other biosorbents [45].

4. Conclusions

The methodology proposed in the present work has permitted the simultaneous and automated monitoring of multicomponent biosorption processes as a general procedure in environmental applications. In this sense, multimetal mixtures of polluting heavy metals have been sorbed on vegetable wastes and the involved ion-exchange processes have been monitored by an automated and real-time prototipe based on flow-injection potentiometry (FIP) and electronic tongue detection (ET). It has been demonstrated that electronic tongues are an appropriate tool for simultaneous measurements in the monitoring of flow processes; by employing the ET, it was accomplished the monitoring of three and four metals simultaneously, by using an array up to a maximum of 9 flow-through cross-response sensors, plus an artificial neural network response model. The cross-response to Cu^{2+}, Cd^{2+}, Zn^{2+}, Pb^{2+} and Ca^{2+} was used to build the ET, but considering the complexity of the studied multimetal processes, a more elaborated approach, viz. the dynamic treatment of the kinetic components of the signal has been needed. The novelty of this procedure results in extracting dynamic components of the peak transient by employing Fourier treatment, and to use the selected coefficients to feed the artificial neural network response model. The performance of grape stalks from wine industry wastes as multimetal biosorbent in fixed bed columns was evaluated, following the indicated procedure, and real-time monitoring of different binary (Cu^{2+}/Pb^{2+}), (Cu^{2+}/Zn^{2+}) and ternary mixtures ($Cu^{2+}/Pb^{2+}/Zn^{2+}$), ($Cu^{2+}/Zn^{2+}/Cd^{2+}$), simultaneous to the release of Ca^{2+} in the effluent solution, was achieved satisfactorily using the reported ET–FIP system. After data processing, the corresponding breakthrough curves were obtained, showing the ion-exchange mechanism among the different metals, as well as the order of affinity of grape stalks for the 4 metals studied corresponds to: $Pb^{2+} > Cu^{2+} > Zn^{2+} \geq Cd^{2+}$. Moreover, analytical performances were verified against conventional spectroscopic techniques, with good agreement of the obtained breakthrough curves and relative error (RE) values for all experiments lower than 0.07, which evidences that there are non-significant differences between the proposed method (ET–FIP) and the reference methods. The results obtained in this study showed that the ET–FIP method is a powerful tool to monitor online and at real time the removal and recovery of heavy metals and can be of great interest in industrial wastewater treatment and processes.

Acknowledgments

This work was supported by MICINN (Spanish Ministry of Science and Innovation), projects CTM2008-06776-C02-02 and CTQ2010-17099; by MINECO (Spanish Ministry of Economy and Competitiveness), CTM2012-37215-C02-02; by program ICREA Academia and by the Catalan government, project 2009SGR905. D. Wilson gratefully acknowledges the concession of a PhD grant by the Universitat Autònoma de Barcelona. Authors also thank A.J. Gago and A. Hernández for helping in part of the experimental work and C. Gauchia for the analysis of samples.

References

[1] N. Fiol, C. Escudero, I. Villaescusa, Bioresour. Technol. 99 (2008) 5030–5036.
[2] C. Valderrama, J.A. Arévalo, I. Casas, M. Martínez, N. Miralles, A. Florido, J. Hazard. Mater. 174 (2010) 144–150.
[3] A. Florido, C. Valderrama, J.A. Arévalo, I. Casas, M. Martínez, N. Miralles, Chem. Eng. J. 156 (2010) 298–304.
[4] N. Miralles, C. Valderrama, I. Casas, M. Martinez, A. Florido, J. Chem. Eng. Data 55 (2010) 3548–3554.
[5] M. Martínez, N. Miralles, S. Hidalgo, N. Fiol, I. Villaescusa, J. Poch, J. Hazard. Mater. 133 (2006) 203–211.
[6] D. Wilson, M. del Valle, S. Alegret, C. Valderrama, A. Florido, Talanta 93 (2012) 285–292.
[7] A. Florido, C. Valderrama, S. Nualart, L. Velazco-Molina, O.A. de Fuentes, M. del Valle, Anal. Chim. Acta 668 (2010) 26–34.
[8] Y. Vlasov, A. Legin, A. Rudnitskaya, C.D. Natale, A. D'Amico, Pure Appl. Chem. 77 (2005) 1965–1983.
[9] M. del Valle, Electroanalysis 22 (2010) 1539–1555.
[10] L. Moreno, J.P. Kloock, M.J. Schöning, A. Baldi, A. Ipatov, A. Bratov, C. Jiménez-Jorquera, Analyst 133 (2008) 1440–1448.
[11] M. Gutiérrez, A. Llobera, J. Vila-Planas, F. Capdevila, S. Demming, S. Büttgenbach, S. Mínguez, C. Jiménez-Jorquera, Analyst 135 (2010) 1718–1725.
[12] D. Wilson, M.N. Abbas, A.L.A. Radwan, M. del Valle, Sensors 11 (2011) 3214–3226.
[13] D. Calvo, A. Durán, M. del Valle, Anal. Chim. Acta 600 (2007) 97–104.
[14] X. Cetó, F. Céspedes, M.I. Pividori, J.M. Gutiérrez, M. del Valle, Analyst 137 (2012) 349–356.
[15] M. del Valle, in: S. Alegret, A. Merkoci (Eds.), Electrochemical Sensor Analysis, Elsevier, Amsterdam, 2007, pp. 721–753.
[16] A. Rudnitskaya, A. Legin, J. Ind. Microbiol. Biotechnol. 35 (2008) 443–451.
[17] M. Gutiérrez, S. Alegret, R. Cáceres, J. Casadesús, O. Marfa, M. del Valle, J. Agric. Food Chem. 56 (2008) 1810–1817.
[18] C.C. Chang, B. Saad, M. Surif, M.N. Ahmad, A.Y.M. Shakaff, Sensors 8 (2008) 3665–3677.
[19] L. Moreno, A. Merlos, N. Abramova, C. Jiménez, A. Bratov, Sens. Actuators B 116 (2006) 130–134.
[20] M.J. Gismera, S. Arias, M.T. Sevilla, J.R. Procopio, Electroanalysis 21 (2009) 979–987.
[21] A. Mimendia, A. Legin, A. Merkoçi, M. del Valle, Sens. Actuators B 146 (2010) 420–426.
[22] Y. Vlasov, A. Legin, Fresenius J. Anal. Chem. 361 (1998) 255–260.
[23] A. Gutés, F. Céspedes, M. del Valle, Anal. Chim. Acta 600 (2007) 90–96.
[24] J. Mortensen, A. Legin, A. Ipatov, A. Rudnitskaya, Y. Vlasov, K. Hjuler, Anal. Chim. Acta 403 (2000) 273–277.
[25] J. Gallardo, S. Alegret, M. del Valle, Sens. Actuators B 101 (2004) 72–80.
[26] F. Lanter, D. Erne, D. Ammann, W. Simon, Anal. Chem. 52 (1980) 2400–2402.
[27] A.J. Frend, G.J. Moody, J.D.R. Thomas, B.J. Birch, Analyst 108 (1983) 1072–1081.

[28] S. Kamata, K. Onoyama, Anal. Chem. 63 (1991) 1295–1298.
[29] D. Wilson, M. Arada, S. Alegret, M. del Valle, J. Hazard. Mater. 181 (2010) 140–146.
[30] R. Kojima, S. Kamata, Anal. Sci. 10 (1994) 409–412.
[31] J.K. Schneider, P. Hofstetter, E. Pretsch, D. Ammann, W. Simon, Helv. Chim. Acta 63 (1980) 217–224.
[32] D. Xu, T. Katsu, Talanta 51 (2000) 365–371.
[33] S. Alegret, A. Florido, J.L.F.C. Lima, A.A.S.C. Machado, Talanta 63 (1989) 825–829.
[34] J. Alonso, J. Baró, J. Bartrolí, J. Sànchez, M. del Valle, Anal. Chim. Acta 308 (1995) 115–121.
[35] V.V. Goud, K. Mohanty, M.S. Rao, N.S. Jayakumar, Chem. Eng. Technol. 28 (2005) 991–997.
[36] C. Valderrama, J. Barios, A. Farran, J.L. Cortina, Water Air Soil Pollut. 215 (2011) 285–297.
[37] V.C. Srivastava, I.D. Malla, I.M.i Mishra, Chem. Eng. Process. 48 (2009) 370–379.
[38] M. Gutiérrez, V.M. Moo, S. Alegret, L. Leija, P.R. Hernández, R. Muñoz, M. del Valle, Microchim. Acta 163 (2008) 81–88.
[39] Y. Umezawa, P. Buhlmann, K. Umezawa, K. Tohda, S. Amemiya, Pure Appl. Chem. 72 (2000) 1851–2082.
[40] M. Cortina, A. Duran, S. Alegret, M. del Valle, Anal. Bioanal. Chem. 385 (2006) 1186–1194.
[41] J. Gallardo, S. Alegret, R. Munoz, L. Leija, P.R. Hernandez, M. del Valle, Electroanalysis 17 (2005) 348–355.
[42] M.M. Figueira, B. Volesky, K. Azarian, V.S.T. Ciminelli, Environ. Sci. Technol. 34 (2000) 4320–4326.
[43] G. Naja, B. Volesky, Physicochem. Eng. Aspects 281 (2006) 194–201.
[44] A.H. Hawari, C.N. Mulligan, Process Biochem. 42 (2007) 1546–1552.
[45] D. Kratochvil, B. Volesky., Water Res. 34 (2000) 3186–3196.
[46] I. Nuic, M. Trgo, J. Peric, N. Vukojevic, Microporous Mesoporous Mater. 167 (2013) 55–61.
[47] E. Escudero, J. Poch, I. Villaescusa, Chem. Eng. J. 217 (2013) 129–138.